Broadband Silicon Four-Mode (De)Multiplexer Using Subwavelength Grating-Assisted Triple-Waveguide Couplers

Weifeng Jiang, Jinzhu Hu, Siqiang Mao, Hanyu Zhang, Linjie Zhou, *Member, IEEE,* and B. M. Azizur Rahman, *Life Fellow, IEEE, Fellow, OSA, Fellow, SPIE*

***Abstract*—A broadband silicon four-mode (de)multiplexer [(De)MUX] is proposed and experimentally demonstrated based on subwavelength gratings (SWGs)-assisted triple-waveguide couplers (TWCs), which can (de)multiplex TE_0, TE_1, TE_2, and TE_3 modes. The mode interaction is enhanced, benefitting from both the triple-waveguide coupling and subwavelength structures. The proposed four-mode (De)MUX is composed of three SWG-assisted TWCs connected by three linear tapers. The experimental results show that the 3-dB bandwidths are 100 nm, 76 nm, 90 nm, and 95 nm for the TE_0, TE_1, TE_2, and TE_3 modes, respectively. The corresponding insertion losses are 0.2, 1.8, 1.3, and 1.7 dB, and the mode crosstalks are -23.3, -17.7, -15.5, and -17.0 dB at the 1550 nm wavelength. The proposed device can work as a mode-(De)MUX compatible with wavelength division multiplexing (WDM) to increase the transmission capacity of on-chip optical interconnects.**

***Index Terms*—Mode division multiplexing, mode (de)multiplexer, subwavelength grating**

I. Introduction

On-chip mode division multiplexing (MDM) has attracted broad attention within the past decade to increase the communication capacity of optical communications and interconnects [1]. The MDM is compatible with the wavelength division multiplexing (WDM) by multiplexing operating-modes over the WDM grids. For a multi-dimensional optical transmission system, a broadband mode (de)multiplexer [(De)MUX] is critical for future robust optical networks [2]. Silicon photonics has proved to be an effective technology for achieving a mode (De)MUX because of its compact footprint from the high refractive index contrast and the complementary metal-oxide-semiconductor (CMOS) compatible fabrication process [3].

To achieve a high-performance on-chip mode (De)MUX, various structures have been considered, including the adiabatic coupler (AC) [4], multimode interference (MMI) coupler [5], asymmetric Y-branch [6], densely packed waveguide arrays (DPWAs) [7], inverse designed structure [8], micro-ring resonator (MRR) [9], and asymmetric directional coupler (ADC) [10]. Amongst these, the AC and MMI couplers can achieve a broadband and fabrication-tolerant mode (De)MUX based on the mode-evolution principle [4,5]. However, these two structures suffer from a large footprint and are also not easy to scale to handle high-order modes. Although an asymmetric Y-branch can be used to form a broadband and low-crosstalk mode (De)MUX, it is not trivial to fabricate the tiny gap between two branches and a long length is also needed for mode evolution [6].

To achieve a compact mode (De)MUX, DPWAs, inverse designed structure, MRR, and ADC could be used [7-10]. The DPWAs can be used to build a broadband and compact mode (De)MUX, but the operating modes are limited. The inverse designed structures are limited by the tight fabrication-tolerance, and the MRR based mode (De)MUXs suffer from the narrow bandwidth. The ADC structure has shown a great promise for large-scale mode (de)multiplexing, benefitting from its high scalability and simple structure. However, the critical phase-matching condition is quite strict for ADC-based mode (De)MUXs. Besides, the bandwidth is limited and the fabrication tolerance is also tight. To relax the phase-matching condition, several performance-enhanced ADC structures have been proposed, including the grating assisted coupler [11], coupled vertical gratings [12], tapered ADC [13], and subwavelength grating (SWG) based ADC [14]. Among these, the SWG-based ADC could form an ultra-broadband mode

This work was supported in part by the National Natural Science Foundation of China under Grant 11904178, in part by the Natural Science Foundation of Jiangsu Province under Grant BK20180743, in part by the NUPTSF under Grant NY218108 and Grant NY219048, and in part by the Research Center of Optical Communications Engineering & Technology, Jiangsu Province under Grant No. ZXF201801. *(Corresponding author: Weifeng Jiang.)*

Weifeng Jiang, Jinzhu Hu, and Siqiang Mao are with the College of Electronic and Optical Engineering, Nanjing University of Posts and Telecommunications, Nanjing 210023, China. (email: jwf@njupt.edu.cn; 1220024229@njupt.edu.cn; 1020020719@njupt.edu.cn).

Hanyu Zhang is with the Peter Grünberg Research Center, College of Telecommunications and Information Engineering, Nanjing University of Posts and Telecommunications, Nanjing 210003, China. (email: hanyu.zhang@njupt.edu.cn).

Linjie Zhou is with the State Key Laboratory of Advanced Optical Communication Systems and Networks, Shanghai Institute for Advanced Communication and Data Science, Department of Electronic Engineering, Shanghai Jiao Tong University, Shanghai 200240, China. (email: ljzhou@sjtu.edu.cn).

B. M. Azizur Rahman is with the Department of Electrical and Electronic Engineering, City, University of London, Northampton Square, London EC1V OHB, UK. (email: B.M.A.Rahman@city.ac.uk).

(De)MUX because the SWG can tailor the dispersion properties of the ADC.

A fabrication-tolerant 11-mode (De)MUX with the low crosstalk between −15.4 dB to −26.4 dB has been experimentally demonstrated using cascaded SWG-based ADCs [14]. A broad bandwidth of ~120 nm has been theoretically achieved for a two-mode (De)MUX via an SWG-based ADC [15]. Besides, two broadband mode (De)MUXs have been experimentally demonstrated based on the SWG engineered MMI coupler [16], and SWG-slot assisted AC [17], which achieves a broad bandwidth of >100 nm. To further increase the bandwidth, we proposed and optimized a two-mode (De)MUX based on a triple-waveguide ADC incorporating a SWG structure, which can numerically achieve an ultra-broad 3-dB bandwidth of 320 nm [18].

In this paper, we extend our original concept of the SWG-assisted triple-waveguide coupler (TWC) to demonstrate a broadband four-mode (De)MUX. The coupling strength is significantly enhanced via both the triple-waveguide coupling and subwavelength structures, and thereby a broad bandwidth is achieved in (de)multiplexing the TE_0, TE_1, TE_2, and TE_3 modes. The proposed four-mode (De)MUX was optimized by using the three-dimensional full-vectorial finite-difference time-domain (3D-FV-FDTD) based band-diagram and propagation analyses. The optimized device was fabricated on the silicon-on-insulator (SOI) platform and experimentally measured.

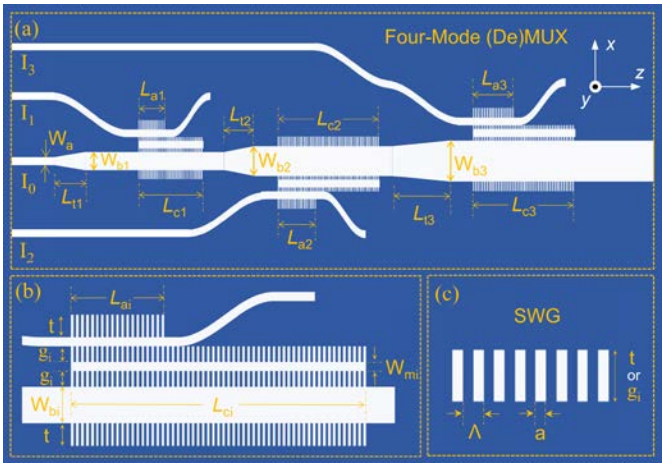

Fig. 1. (a) Structure of the proposed silicon four-mode (De)MUX. (b) Three-waveguide coupler incorporating subwavelength gratings. (c) Subwavelength grating.

II. Results

A. Structure and Operating Principle

The schematic structure of the proposed silicon four-mode (De)MUX is shown in Fig. 1(a), consisting of three SWG-assisted TWCs connected by three linear tapers. The fundamental TE modes are launched from ports I_0, I_1, I_2, and I_3, which are then multiplexed to the TE_0, TE_1, TE_2, and TE_3 modes of the bus waveguide by using the tapers and three TWCs. The enlarged TWC-structure is shown in Fig. 1(b). Three strip waveguides are embedded in four rows of SWGs. The extents of two outside SWGs are denoted by t, and those of two inside SWGs are denoted by g_i, where i = 1, 2, and 3 for 1st, 2nd, and 3rd [from left to right in Fig. 1(a)] TWCs, respectively. The pitch and duty cycle of SWG are denoted as Λ and $f = a/\Lambda$, respectively, as shown in Fig. 1(c). The coupling strength of the TWC can be significantly increased benefitting from the SWG structures, and thereby a short coupling length and a broad bandwidth are expected. As shown in Figs. 1(a) and 1(b), the coupling length and the width of the middle waveguide are denoted as L_{ci} and W_{mi}, respectively. The length of the SWG-based straight access-waveguide is represented by L_{ai}. The width of the bus waveguide is denoted as W_{bi}, where i = 1, 2, and 3 for 1st, 2nd, and 3rd TWCs, respectively. In this case, the 1st, 2nd, and 3rd TWCs are capable of (de)multiplexing the TE_1, TE_2, and TE_3 modes, respectively. The lengths of three tapers for connecting bus-waveguides are denoted as L_{t1}, L_{t2}, and L_{t3}. The width of the access waveguides is denoted as W_a.

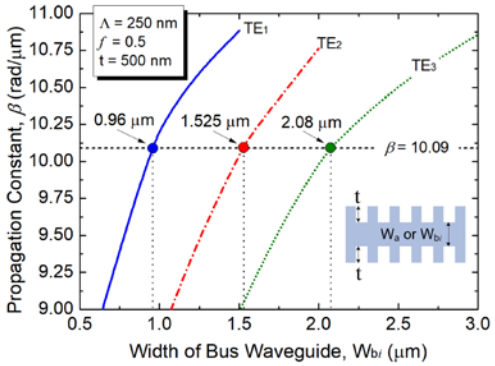

Fig. 2. Phase-matching conditions for TE_1, TE_2, and TE_3 modes of the SWG-based bus waveguides.

B. Phase-Matching and Optimizations

As the TE_1, TE_2, and TE_3 modes are coupled via the 1st, 2nd, and 3rd TWCs, respectively, the phase-matching conditions of three TWCs are investigated for these three modes. In this case, the phase-matched width of the bus waveguide is determined by optimizing the individual SWG access and bus waveguides, and then the phase-matched width of the middle waveguide is optimized according to the propagation characteristics of the combined TWC. To obtain the phase-matched width of the bus waveguide, the propagation constants of the SWG access and bus waveguides are calculated by using the 3D-FV-FDTD based band-diagram calculations with Bloch boundary condition [19]. Variations of the propagation constant at 1550 nm with the bus waveguide width are shown in Fig. 2. The simulated structure of the SWG waveguide is shown in the inset of Fig. 2. In the simulations, the pitch and duty-cycle of the SWG are chosen to be Λ = 250 nm and f = 0.5, respectively. The extent of SWG is set as t = 500 nm, with symmetric refractive index distribution on both sides [18]. The refractive indices of silicon and silica are referred to the Palik's book [20]. The thickness of the silicon layer is 220 nm and the width of the access waveguide is W_a = 400 nm. The propagation constant of the SWG access waveguide is calculated to be 10.09, as indicated by the horizontal black dashed line in Fig. 2. The propagation constants of the TE_1, TE_2, and TE_3 modes in the SWG bus waveguides are represented by blue solid, red dash-dotted, and green dotted lines, respectively. The phase-matched

widths of the bus waveguides are calculated to be W_{b1} = 0.96 μm, W_{b2} = 1.525 μm, and W_{b3} = 2.08 μm for the 1st, 2nd, and 3rd TWCs, respectively.

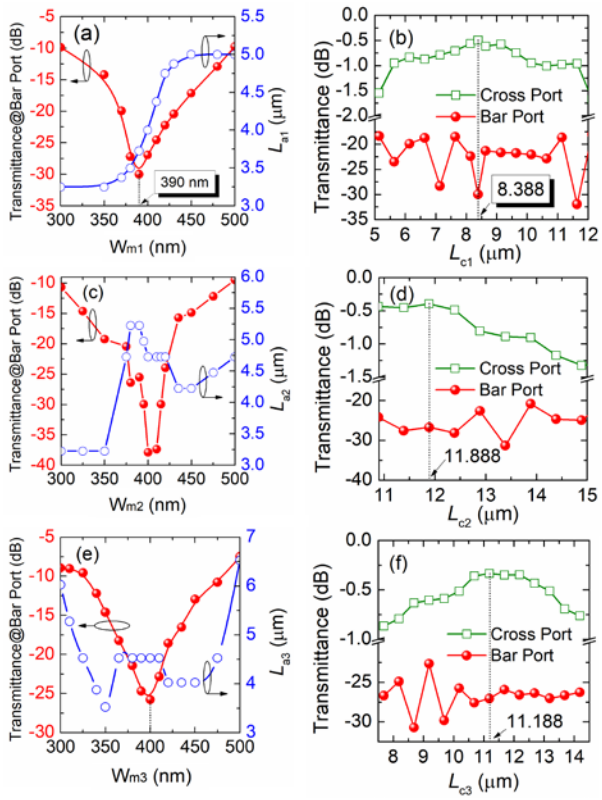

Fig. 3. Variations of the transmittance at the bar port (left *y*-axis) and optimized length of the SWG based straight access-waveguide (right *y*-axis) with the middle-waveguide width, (a) W_{m1}, (c) W_{m2}, and (e) W_{m3}, respectively. Variations of the transmittance with the coupling length, (b) L_{c1}, (d) L_{c2}, and (f) L_{c3}, respectively.

Next, the phase-matched width of the middle-waveguide is optimized by varying the coupling length, L_{ci}, and the length of the SWG access waveguide, L_{ai}. It should be noted that the TWCs are simulated individually. The coupling length is firstly kept constant, and the minimum power at the bar port is obtained by optimizing W_{mi} and L_{ai}. Then, the optimized W_{mi} and L_{ai} are kept constant and the coupling length, L_{ci}, is varied to achieve the maximum power at the cross port. Variations of the transmittance at the bar port (left *y*-axis) and optimized L_{ai} (right *y*-axis) with the middle waveguide width, W_{mi}, are shown in Figs. 3(a), 3(c), and 3(e). In the calculations, the gap between three waveguides is set to be g_i = 200 nm for three TWCs. For the access waveguide of each TWC, input and output S-bend waveguides with the sizes of 10 μm × 2 μm and 5 μm × 2 μm are used to decouple SWG waveguides. To reduce the mode transition loss, two straight segments with the lengths of 1.5 and 0.5 μm are inserted between the input/output S-bends and SWG access waveguide. Initially, the coupling lengths are set as L_{c1} = 8.4 μm, L_{c2} = 8.9 μm, and L_{c3} = 10.2 μm in Figs. 3(a), 3(c), and 3(e). The optimized middle waveguide widths are W_{m1} = 390 nm, W_{m2} = 400 nm, and W_{m3} = 400 nm and the corresponding L_{ai} are calculated to be L_{a1} = 3.725 μm, L_{a2} = 4.725 μm, and L_{a3} = 4.525 μm.

Variations of the transmittance with the coupling length are then calculated and shown in Figs. 3(b), 3(d), and 3(f). The optimized coupling lengths are identified as L_{c1} = 8.388 μm, L_{c2} = 11.888 μm, and L_{c3} = 11.188 μm, which gives the maximum output at the cross port. The insertion losses are calculated to be 0.5, 0.4, and 0.3 dB, and the crosstalks are -29.5, -26.3, and -26.7 dB for 1st, 2nd, and 3rd TWCs, respectively. The propagation fields along the z-direction are simulated by using the 3D-FV-FDTD method and shown in Figs. 4(a)-4(c) for multiplexing the TE_1, TE_2, and TE_3 modes, respectively. It can be observed that the launched TE_0 modes from the access waveguides can be completely converted to the TE_1, TE_2, and TE_3 modes, respectively. As the output field is composed of mixed modes, the output power of each high-order mode is analyzed by using the mode expansion method (MEM). The lengths of three tapers connecting the bus waveguides are also optimized and chosen to be L_{t1} =4.5 μm, L_{t2} = 8.5 μm, and L_{t3} =4.5 μm, respectively, and the excess losses are lower than 0.003 dB.

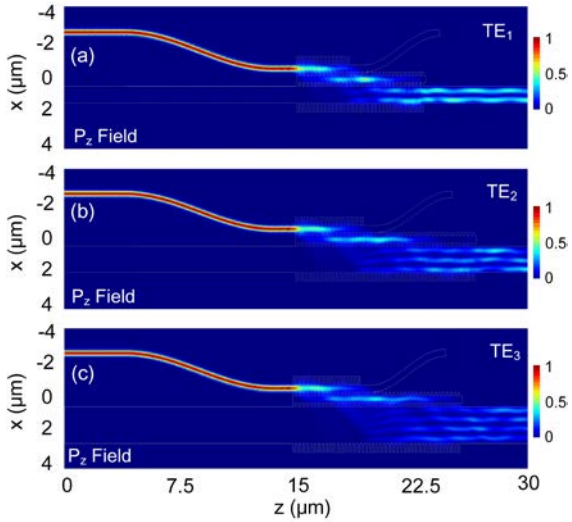

Fig. 4. Propagation fields along the z-direction for multiplexing (a) TE_1, (b) TE_2, and (c) TE_3 modes.

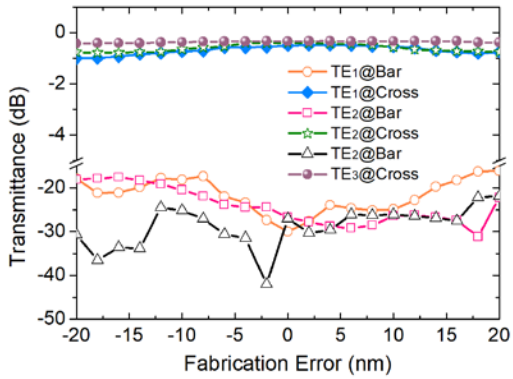

Fig. 5. Fabrication tolerance of the optimized four-mode (De)MUX.

The tolerances and robustness of optimized four-mode (De)MUX to the fabrication error are analyzed by using the 3D-FV-FDTD method. To perform a trustworthy tolerance study, the fabrication errors were applied to both the *x* and *z* directions. Hence, the duty cycle was varied according to the width changes along the *z* direction. The widths of three waveguides were simultaneously changed according to the width changes

along the *x* direction. In this case, the deterioration of the performance of the SWG-assisted TWC mostly depends on the change of the duty cycle. The fabrication errors of ±20 nm of the width changes along the *z* direction are corresponding to the ±16% pitch fractional error. Variations of the transmittance with the fabrication error are shown in Fig. 5. With the fabrication error of ± 20 nm, the degradations of the insertion loss are less than 0.5, 0.39, and 0.1 dB for 1st, 2nd, and 3rd TWCs, respectively. The mode crosstalks are less than -15.4, -16.8, and -21.5 dB for the fabrication error of ± 20 nm. In addition, the performances on the fabrication error over a 100-nm bandwidth were also calculated and the results are as follows: when the widths of access, middle, and bus guides, and extents of two outside SWGs are simultaneously changed by -20 nm (+20 nm), the mode crosstalks over the wavelength ranging from 1.5 to 1.6 μm are less than -7.2 (-11.8), -19.2 (-22.7), and -20.7 (-17.8) dB for coupling the TE_1, TE_2, and TE_3 modes, respectively. When the duty cycle of SWG is changed by -8% (+8%), the mode crosstalks over the wavelength ranging from 1.5 to 1.6 μm are less than -7.8 (-10.14), -15.6 (-21.8), and -15.8 (-22.6) dB for coupling the TE_1, TE_2, and TE_3 modes, respectively. We can see that the mode crosstalk of our proposed mode (De)MUX is mainly limited to the first TWC for coupling the TE_1 mode. Hence, the measured performance will be better by changing the parameters of first TWC. The mode conversion can be taken place at the waveguide junction. The light backscattering loss could be generated when the SWG arrays are suddenly introduced in the TWC section. If the grating extends are tapered at the connection, a smooth transition from silicon waveguides without SWGs to that with the SWGs can be achieved. Therefore, the operating mode is not see sudden change in waveguide, and backscattering loss and mode crosstalk would be reduced.

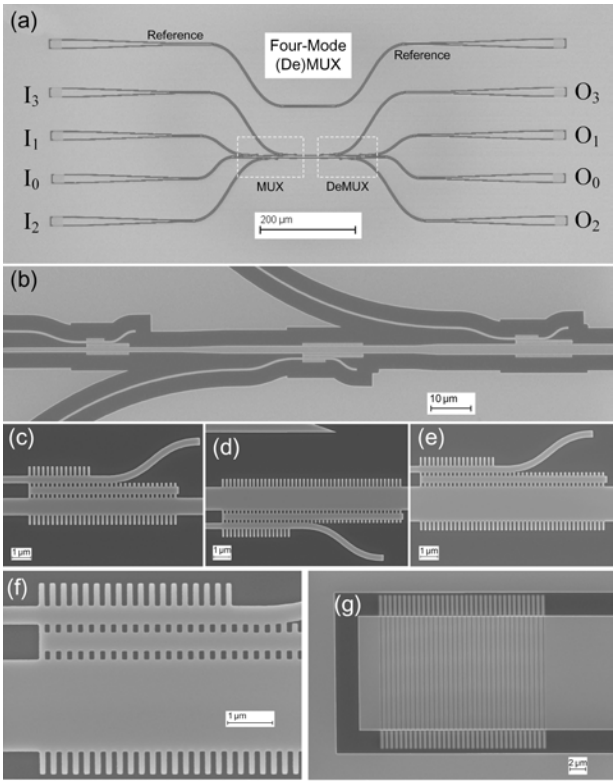

Fig. 6. (a) SEM image of the fabricated four-mode (De)MUX. (b) Coupling regions for multiplexing three modes. Three-waveguide couplers incorporating SWGs for multiplexing (c) TE_1, (d) TE_2, and (e) TE_3 modes. (f) Zoom-in image of the SWG coupling region. (g) Enlarged image of the grating coupler.

C. Fabrication and Experimental Measurements

The optimized four-mode (De)MUX was fabricated on an SOI wafer with a 220-nm-thick silicon layer and a 3-μm buried oxide (BOX) layer. The device was patterned by using the electron beam lithography (EBL, Vistec EBPG 5200+) and then etched via inductively coupled plasma (ICP, SPTS DRIE-I). A 1-μm-thick silica cladding was finally deposited by using the plasma-enhanced chemical vapor deposition (PECVD, Oxford). The scanning electron microscope (SEM, ZEISS) image of the fabricated four-mode (De)MUX is shown in Fig. 6(a), including both a four-mode MUX and a four-mode DeMUX. The SEM image of the four-mode MUX section is shown in Fig. 6(b). SWG-assisted TWCs for multiplexing TE_1, TE_2, and TE_3 modes are shown in Figs. 6(c)-6(e), respectively. The Zoom-in image of the SWG coupling region is shown in Fig. 6(f). A reference waveguide with input/output grating couplers (GCs) was also fabricated, as shown in Fig. 6(a). The pitch and duty cycle of the TE_0-mode GCs are 630 nm and 0.48, respectively, and the etching depth is 70 nm. The enlarged image of the GC is shown in Fig. 6(g). A polarization controller is connected to a tunable laser to set TE-polarization of the input light.

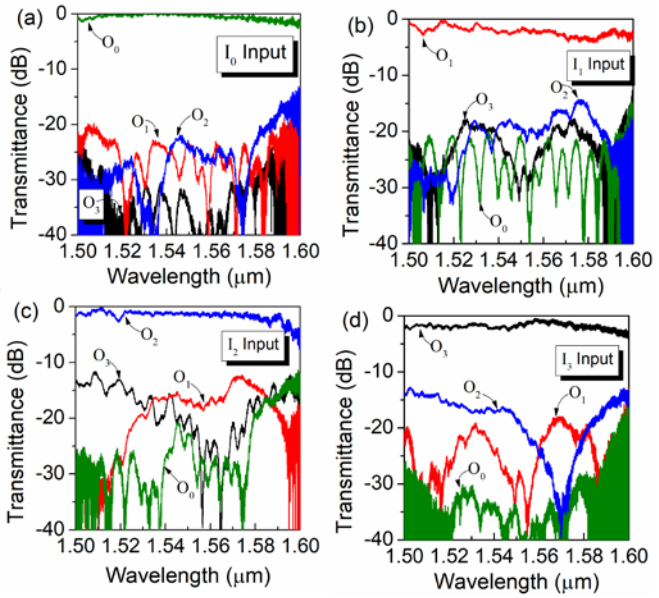

Fig. 7. Measured transmission spectra at four output ports when light is launched from the input port (a) I_0, (b) I_1, (c) I_2, and (d) I_3.

triple-waveguide coupling. The bandwidths of all modes can fully cover the C-band in WDM networks. Thus, the proposed mode (De)MUX can be implemented in a hybrid MDM-WDM network. As the sizes of mode fields are different for different modes, the evanescent fields would also be different. The different bandwidths could be due to different mode-coupling strengths for different modes. The waveguide widths of TWCs can be changed to improve the operating bandwidths. Note that the device performance can be further improved by reducing the fabrication error.

Table I compares the experimental performance and length of our fabricated device with that of the reported mode (De)MUXs. It can be noted that the adiabatic coupler based mode (De)MUX has reported a relatively large bandwidth, a low loss, and a low crosstalk, but a relatively long length of several hundred micrometers. The architecture based on MMI coupler shows a broad bandwidth, but the operating modes are limited. The asymmetric Y-junction provides a high crosstalk value and its fabrication problems would be critical due to the limited resolution of the tiny gap mentioned in the Introduction

TABLE I
EXPERIMENTAL PERFORMANCE AND LENGTH OF REPORTED MODE (DE)MUXS

Architecture	N_{ch}	Length (μm)	Insertion Loss (dB)	Crosstalk (dB)	Bandwidth (nm)	Ref./ Year
Adiabatic coupler	3	310	~0.2	<-18.0	65	[4]/2017
MMI coupler	2	68	5.5~7.3	/	100	[5]/2018
Y-branch	3	>320	<5.7	<-9.7	29	[6]/2016
DPWAs	3	60	0.6	<-15	80	[7]/2015
Inverse design	3	~5	<1.0	<-20	80	[8]/2019
Micro-ring resonator	3	~250	1.5	<-12	<5.0	[9]/2014
Coupled vertical gratings	3~5	500	<2.0	-5~-20	<15	[12]/2015
Tapered ADC	2	44.11	<1.0	<-17.4	C+L	[13]/2019
SWG based ADCs	11	217.9	<5.2	<-10	50	[14]/2018
SWG based MMI coupler	2	38.6	<1.1	<-18	120	[16]/2020
SWG-slot assisted AC	2	55	<2.6	<18.8	230	[17]/2020
This work	4	48.964	<5.0	<-10.0	100	

The measured transmittance responses at four output ports are shown in Figs. 7(a)-7(d) when input is from I_0, I_1, I_2, and I_3, respectively. The transmission spectra were normalized to that of the reference waveguide shown in Fig. 6(a). The measured insertion losses at 1550 nm are 0.2, 1.8, 1.3, and 1.7 dB and the mode crosstalks are -23.3, -17.7, -15.5, and -17.0 dB, when the input port is I_0, I_1, I_2, and I_3 to (de)multiplex TE_0, TE_1, TE_2, and TE_3 modes, respectively. Compared to the simulated results, the measured loss is a little bit high due to the imperfection of the fabrication process. The 3-dB bandwidths are measured to be 100 nm, 76 nm, 90 nm, and 95 nm for inputs I_0, I_1, I_2, and I_3, respectively. For the wavelength range from 1.5 μm to 1.6 μm, the mode crosstalk is less than -15.0 dB for input ports I_0 and I_1 and less than -10.0 dB for input ports I_2 and I_3. It reveals that the fabricated four-mode (De)MUX has a broadband response for all modes, benefitting from both the SWG structures and section. Although the structure based on DPWAs achieves a relatively broad bandwidth and a low loss, the performances of the device length and operating modes need to be improved. The inverse designed structure shows a compact footprint and a relatively large bandwidth, but its fabrication-tolerance is tight. The architectures based on the MRR and coupled vertical gratings are limited by a narrow bandwidth. The tapered ADC achieves a relatively broad bandwidth and a low loss, but its device length would be larger compared to the SWG based structures. The SWG assisted ADCs, MMI couplers, and ACs shows a broad bandwidth and a compact length. Despite the imperfection of the fabrication process, our device exhibits a broad bandwidth and a compact length. In this work, the four-mode (De)MUX is considered, but the proposed mode (De)MUX can be scaled up for even higher order modes.

III. Conclusion

In conclusion, we have proposed and experimentally demonstrated a four-mode (De)MUX based on three SWG-assisted TWCs. The band diagram of the SWG waveguides and the propagation characteristics were calculated by using the 3D-FV-FDTD method. The experimental results show that the fabricated four-mode (De)MUX has low insertion losses (crosstalks) of 0.2 (-23.3), 1.8 (-17.7), 1.3 (-15.5), and 1.7 (-17.0) dB for (de)multiplexing the TE_0, TE_1, TE_2, and TE_3 modes, respectively. The 3-dB bandwidths of 100 nm, 76 nm, 90 nm, and 95 nm have been achieved for the four TE modes, respectively. The proposed mode (De)MUX can be applied to on-chip MDM-WDM systems, increasing the communication capacity of each WDM channel.

References

[1] X. Wu, C. Huang, K. Xu, C. Shu, and H. K. Tsang, "Mode-division multiplexing for silicon photonic network-on-chip," *J. Lightw. Technol*., vol. 35, no. 15, pp. 3223-3228, Aug. 2017.

[2] D. Dai, C. Li, S. Wang, H. Wu, Y. Shi, Z. Wu, S. Gao, T. Dai, H. Yu, and H. K. Tsang, "10-channel mode (de)multiplexer with dual polarizations," *Laser Photon. Rev*., vol. 12, no. 1, Jan. 2018, Art. no. 1700109.

[3] C. Li, D. Liu, and D. Dai, "Multimode silicon photonics," *Nanophotonics*, vol. 8, no. 2, pp. 227-247, Feb. 2019.

[4] C. Li and D. Dai, "Low-loss and low-crosstalk multi-channel mode (de)multiplexer with ultrathin silicon waveguides," *Opt. Lett*., vol. 42, no. 12, pp. 2370-2373, Jun. 2017.

[5] R. B. Priti and O. Liboiron-Ladouceur, "A reconfigurable multimode demultiplexer/switch for mode-multiplexed silicon photonics interconnects," *IEEE J. Sel. Top. Quantum Electron*., vol. 24, no. 6, Nov/Dec. 2018, Art. no. 8300810.

[6] W. Chen, P. Wang, T. Yang, G. Wang, T. Dai, Y. Zhang, L. Zhou, X. Jiang, and J. Yang, "Silicon three-mode (de)multiplexer based on cascaded asymmetric Y junctions," *Opt. Lett*., vol. 41, no. 12, pp. 2851-2854, Jun. 2016.

[7] K. Chen, S. Wang, S. Chen, S. Wang, C. Zhang, D. Dai, and L. Liu, "Experimental demonstration of simultaneous mode and polarization-division multiplexing based on silicon densely packed waveguide array," *Opt. Lett*., vol. 40, no. 20, pp. 4655-4658, Oct. 2015.

[8] Y. Liu, K. Xu, S. Wang, W. Shen, H. Xie, Y. Wang, S. Xiao, Y. Yao, J. Du, Z. He, and Q. Song, "Arbitrarily routed mode-division multiplexed photonic circuits for dense integration," *Nat. Commun*., vol. 10, Jul. 2019, Art. no. 3263.

[9] L.-W. Luo, N. Ophir, C. P. Chen, L. H. Gabrielli, C. B. Poitras, K. Bergmen, and M. Lipson, "WDM-compatible mode-division multiplexing on a silicon chip," N*at. Commun*., vol. 5, Jan. 2014, Art. no. 3069.

[10] W. Jiang, J. Miao, and T. Li, "Compact silicon 10-mode multi/demultiplexer for hybrid mode-and polarisation-division multiplexing system," *Sci. Rep*., vol. 9, no. 1, Sep. 2019, Art. no. 13223.

[11] H. Qiu, H. Yu, T. Hu, G. Jiang, H. Shao, P. Yu, J. Yang, and X. Jiang, "Silicon mode multi/demultiplexer based on multimode grating-assisted couplers," *Opt. Express*, vol. 21, no. 15, pp. 17904-17911, Jul. 2013.

[12] G. F. R. Chen, T. Wang, K. J. A. Ooi, A. K. L. Chee, L. K. Ang, and D. T. H. Tan, "Wavelength selective mode division multiplexing on a silicon chip," *Opt. Express*, vol. 23, no. 6, pp. 8095-8103, Mar. 2015.

[13] H. Shu, B. Shen, Q. Deng, M. Jin, X. Wang, and Z. Zhou, "A design guideline for mode (de)multiplexer based on integrated tapered asymmetric directional coupler," *IEEE Photon. J*., vol. 11, no. 5, Oct. 2019, Art .no. 2941742.

[14] Y. He, Y. Zhang, Q. Zhu, S. An, R. Cao, X. Guo, C. Qiu, and Y. Su, "Silicon high-order mode (de)multiplexer on single polarization," *J. Lightwave Technol*., vol. 36, no. 24, pp. 5746-5753, Dec. 2018.

[15] Z. Jafari, A. Zarifkar, and M. Miri, "Compact fabrication-tolerant subwavelength-grating-based two-mode division (de)multiplexer," *Appl. Opt*., vol. 56, no. 26, pp. 7311-7319, Sep. 2017.

[16] D. González-Andrade, A. Dias, J. G. Wangüemert-Pérez, A. Ortega-Moñux, Í. Molina-Fernández, R. Halir, P. Cheben, and A. V. Velasco, "Experimental demonstration of a broadband mode converter and multiplexer based on subwavelength grating waveguides," *Opt. Laser Technol*., vol. 129, Sep. 2020, Art. no. 106297.

[17] L. Xu, Y. Wang, D. Mao, J. Zhang, Z. Xing, E. El-Fiky, M. G. Saber, A. Kumar,Y. D'Mello, M. Jacques, and D. V. Plant, "Ultra-broadband and compact two-mode multiplexer based on subwavelength-grating-slot-assisted adiabatic coupler for the silicon-on-insulator platform," *J. Lightwave Technol*., vol. 37, no. 23, pp. 5790-5800, Dec. 2019.

[18] W. Jiang, J. Miao, T. Li, and L. Ma, "Ultra-broadband and fabrication-tolerant mode (de)multiplexer using subwavelength structure," *J. Opt. Soc. Am*. B, vol. 36, no. 11, pp. 3125-3132, Nov. 2019.

[19] H. Yun, L. Chrostowski, and N. A. Jaeger, "Ultra-broadband 2 × 2 adiabatic 3 dB coupler using subwavelength-grating-assisted silicon-on-insulator strip waveguides," *Opt. Lett*., vol. 43, no. 8, pp. 1935-1938, Apr. 2018.

[20] E. D. Palik, Handbook of Optical Constants of Solids (Academic, 1998).

Weifeng Jiang received PhD degree in Physics Electronics from Southeast University, Nanjing, China, in 2015. He was a postdoctoral fellow at City, University of London as a postdoctoral fellow from 2015 to 2016. He then joined Nanjing University of Posts and Telecommunications as a lecturer, researching into silicon photonics systems for optical communications and sensing.

Jinzhu Hu is currently working toward the master degree with Nanjing University of Posts and Telecommunications, Nanjing, China focusing on silicon photonics for optical communications and sensing.

Siqiang Mao is currently working toward the master degree with Nanjing University of Posts and Telecommunications, Nanjing, China focusing on silicon photonics for optical communications.

Hanyu Zhang received the B.S. degree in microelectronic manufacturing engineering from Central South University in 2015. She received the Ph.D. degree in electronic science and technology from Shanghai Jiao Tong University in 2020. She is currently a lecturer at the College of Telecommunications and Information Engineering, Nanjing University of Posts and Telecommunications. His research concentrates on fabrication and tests the integration of phase change materials with silicon photonics for optoelectronic or optical computing applications.

Linjie Zhou (M'03) received the B.S. degree in microelectronics from Peking University, Beijing, China, in 2003. He received the Ph.D. degree in electronic and computer engineering from the Hong Kong University of Science and Technology, Hong Kong, in 2007. From 2007 to 2009, he worked as a Postdoctoral Researcher with the University of California, Davis, CA, USA. Currently, he is a Professor with the State Key Lab of Advanced Optical Communication Systems and Networks, Shanghai Jiao Tong University. His research interests include silicon photonics, plasmonic devices, and optical integration.

B. M. Azizur Rahman (S'80–M'83–SM'94–F'16–LF'18) received the B.Sc.Eng and M.Sc.Eng. degrees in Electrical Engineering with distinctions from Bangladesh University of Engineering and Technology (BUET), Dhaka, Bangladesh, in 1976 and 1979, respectively. He also received two gold medals for being the best undergraduate and graduate students of the university in 1976 and 1979, respectively. In 1979, he was awarded with a Commonwealth Scholarship to study for a PhD degree in the UK and subsequently in 1982 received his PhD degree in Electronics from University College London.

In 1988, he joined City University, London, as a lecturer, where became a full Professor in 2000. At City University, he leads the research group on Photonics Modelling, specialised in the development and use of rigorous and full-vectorial numerical approaches to design, analyse and optimise a wide range of photonic devices, such as spot-size converters, high-speed optical modulators, compact bend designs, power splitters, polarisation splitters, polarisation rotators, polarization controllers, SBS, terahertz devices, etc. He has published more than 600 journal and conference papers, and his journal papers have been cited more than 7000 times. He has supervised 34 students to complete their PhD degrees as their first supervisor and received more than £13 M in research grants. Prof. Rahman is Life Fellow of the IEEE, Fellow of the Optical Society of America and the SPIE.